The AAPS Journal, Vol. 16, No. 5, September 2014 (© 2014)
DOI: 10.1208/s12248-014-9626-3

Research Article

Application of a Physiologically Based Pharmacokinetic Model Informed by a Top-Down Approach for the Prediction of Pharmacokinetics in Chronic Kidney Disease Patients

Hiroyuki Sayama,[1,3] Hiroaki Takubo,[1] Hiroshi Komura,[1] Motohiro Kogayu,[1] and Masahiro Iwaki[2]

Received 2 March 2014; accepted 19 May 2014; published online 11 June 2014

Abstract. Quantitative prediction of the impact of chronic kidney disease (CKD) on drug disposition has become important for the optimal design of clinical studies in patients. In this study, clinical data of 151 compounds under CKD conditions were extensively surveyed, and alterations in pharmacokinetic parameters were evaluated. In CKD patients, the unbound hepatic intrinsic clearance decreased to a similar extent for drugs eliminated *via* hepatic metabolism by cytochrome P450, UDP-glucuronosyltransferase, and other mechanisms. Renal clearance showed a similar decrease to glomerular filtration rate, irrespective of the contribution of tubular secretion. The scaling factor (SF) obtained from the interquartile range of the relative change in each parameter was applied to the well-stirred model to predict clearance in patients. Hepatic and renal clearance could be successfully predicted for approximately half and two-thirds, respectively, of the applied compounds, showing the high utility of SFs. SFs were also introduced to a physiologically based pharmacokinetic (PBPK) model, and the plasma concentration profiles of 12 model compounds with different elimination pathways were predicted for CKD patients. The PBPK model combined with SFs provided good predictability for plasma concentration. The developed PBPK model with information on SFs would accelerate translational research in drug development by predicting pharmacokinetics in CKD patients.

KEY WORDS: model-based drug development; modeling and simulation; PBPK; pharmacokinetics; renal impairment.

INTRODUCTION

Chronic kidney disease (CKD) is a worldwide public health problem with global increase in the number of patients (1,2). CKD is associated with multiple physiological changes and, hence, alters the pharmacokinetics (PK) of drugs, which could cause adverse effects (3–5). According to the survey of new molecular entities approved from 2003 to 2007 by the US Food and Drug Administration (FDA), half of the orally administered compounds with altered drug disposition in patients with renal disease were predominantly eliminated by non-renal pathways such as hepatic metabolism or biliary excretion (6). In 2010, the FDA issued a draft guidance emphasizing the need to perform clinical studies on drugs that are eliminated by non-renal mechanisms as well as the renal route in patients with renal impairment (7). For pharmaceutical industries, quantitative prediction of the impact of CKD on drug disposition has become important for the optimal design of clinical studies in patients including careful dosage adjustment to avoid possible side effects.

Recently, physiologically based pharmacokinetic (PBPK) modeling and simulation has increasingly gained importance to provide a rational design for first-in-human studies (8). PBPK modeling is, generally, constructed based on a bottom-up approach, which needs a large number of input parameters such as plasma protein binding and metabolic intrinsic clearance (CL_{intH}), in addition to physicochemical properties and physiological parameters. With regard to hepatic failure, quantitative variations in the activity or content of cytochrome P450 (CYP) enzymes have been reportedly available alongside alternation of physiological parameters, and such information are successfully applied to PBPK models to describe the PK in liver cirrhosis (9,10).

On the other hand, the effects of chronic renal failure (CRF) on PK have been evaluated mainly in animal models (11,12). Based on the accumulated evidence from *in vitro* and *in vivo* studies, the mechanisms underlying the alternation of PK can be explained as follows (3,4): uremic toxins such as indoxyl sulfate, parathyroid hormone, and cytokines, all of which are highly increased in the serum of chronic renal failure patients, are involved in either the transcriptional or

Electronic supplementary material The online version of this article (doi:10.1208/s12248-014-9626-3) contains supplementary material, which is available to authorized users.

[1] Drug Metabolism & Pharmacokinetics Research Laboratories, Central Pharmaceutical Research Institute, Japan Tobacco Inc., Osaka, Japan.
[2] Department of Pharmacy, Faculty of Pharmaceutical Sciences, Kinki University, Osaka, Japan.
[3] To whom correspondence should be addressed. (e-mail: hiroyuki.sayama@jt.com)

translational modifications or direct inhibition of CYP enzymes or transporters. The elevated concentrations of parathyroid hormone in chronic renal failure lead to the down-regulation of hepatic drug-metabolizing enzymes including CYP enzymes through activation processes like nuclear factor-κB. Since various mechanisms are complexly intertwined, it is difficult to quantitatively evaluate these parameters in CKD condition, which are necessary for the bottom-up approach, based on *in vitro* systems and *in vivo* animal models for individual drugs.

Meanwhile, the top-down approach, which is based on the actual changes in PK parameters derived from clinical data, would become a useful tool to predict drug dispositions in CKD patients by the PBPK model. Rowland *et al.* quantitatively estimated the microsomal content of CYP1A2, CYP2C8, CYP2C9, CYP2C19, and CYP3A4 enzymes in CKD condition (13), by the back calculation of *in vivo* hepatic clearance (CL_H) to CL_{intH} including the correction of differences in plasma protein binding, and predicted the PK of paroxetine, diltiazem, and repaglinide in patients. The same input parameters for CYP enzyme abundance in CKD condition were also utilized by Zhao *et al.*, who prepared an expanded PBPK model by incorporating the hepatic uptake process (14). Furthermore, the simulation of the changes in plasma concentrations of solifenacin in CKD patients employed a factor of 0.6, which was estimated from the difference in *in vivo* clearance (CL) between healthy volunteers (HV) and CKD patients (15). Although these PBPK models informed by the top-down approach allow successful predictions of PK in CKD patients for certain drugs, the reduction of CL_{intH} or *in vivo* CL in CKD patients in these models is derived from a limited number of clinical studies.

Importantly, taking complex mechanisms into consideration, a relatively large dataset encompassing an equally large number of drugs is essentially required for the top-down approach, and the change ratios of PK parameters obtained from the differences between CKD patients and HV should be applied as scaling factors (SF) to the prediction of the plasma concentrations in the PBPK model. In the present study, we extensively collected clinical data of CKD patients for a variety of drugs that are non-renally and/or renally eliminated, and the utility of the obtained SFs in the PBPK model was evaluated by comparing the predicted and observed changes in PK parameters and plasma concentration profiles in CKD patients.

MATERIALS AND METHODS

Data Collection

The clinical data for 151 compounds, for which PK parameters in HV and both moderate and severe CKD patients were available, were collected from the literature or the PharmaPendium database (Elsevier, NY, USA; https://www.pharmapendium.com/). Moderate and severe CKD are generally defined by a glomerular filtration rate (GFR); 30 to 59 mL/min/1.73 m^2 for moderate and 15 to 29 mL/min/1.73 m^2 for severe CKD. The collected PK parameters were as follows: unbound fraction in plasma (f_p), fraction excreted unchanged in urine (f_e), an apparent volume of distribution at a steady state (V_{ss}), CL, area under the plasma concentration-time curve (AUC) after oral dosing, and the elimination half-life ($t_{1/2}$). These data were summarized as supplemental data (Supplementary Table S1). *In silico* parameters such as lipophilicity (clogP), pH-dependent measure of lipophilicity (clogD), and basic and acidic dissociation constants (pK_a) were calculated from structural information using CLOGP, version 4.82 (Daylight Chemical Information Systems Inc., CA, USA) and Pallas, version 4.4.1 (CompuDrug Inc., AZ, USA). The compounds were divided into acidic, basic, and neutral classes based on the differences between the clogD values at pH 6.5 and 7.4 (ΔclogD) as indicated by the following equation:

$$\Delta\text{clogD} = \text{clogD}_{\text{pH6.5}} - \text{clogD}_{\text{pH7.4}} \quad (1)$$

Compounds with positive and negative ΔclogD values were classified as acidic and basic, respectively. Compounds with ΔclogD values of zero were assumed to be neutral. As blood to plasma concentration ratio (R_B) values of most compounds were not available from the literature data, they were assumed to be 0.6 for acidic compounds and 1 for the other, basic and neutral, compounds (16–18). Unbound fraction in blood (f_B) was calculated by dividing f_p by R_B. The information on hepatic elimination mechanisms including the contribution of CYP enzymes was obtained from the literature or FDA approval packages.

Dataset for the Evaluation and Prediction of CL Alterations

To evaluate the alteration of unbound CL_{intH} (CL_{UintH}) in disease conditions, the 1st dataset was used as a training set. The 1st dataset consists of PK data after oral administration for 76 compounds that are mainly eliminated *via* the hepatic route (f_e<0.4; averaged value, 0.05). Then, the SF for CL_{UintH} obtained from the 1st dataset was applied to the well-stirred model together with those for f_p and renal blood clearance (CL_R), and predictabilities for CLs in CKD conditions were confirmed using the 2nd dataset as a validation set. The 2nd dataset, which is independent from the 1st dataset, consists of intravenous data of 40 compounds eliminated *via* both renal and non-renal routes (averaged f_e value, 0.50). In addition, within the 2nd dataset, the compounds, for which plasma concentration-time profiles were available, were used for the validation of a PBPK model combined with the SFs in CKD patients. The summary of 1st and 2nd datasets was shown in the supplemental data (Supplementary Table S2).

Alterations of the PK Parameters in CKD Patients

Collected f_p and V_{ss} in patients with moderate and severe CKD were compared with those in HV to produce the relative percentages (RP) for each disease stage as shown in the following equation:

$$\text{RP} = \frac{\text{Parameter in disease condition}}{\text{Parameter in healthy condition}} \times 100 \quad (2)$$

CL_R was obtained from the literature information or calculated from plasma CL after intravenous dosing as shown in the following equation:

$$CL_R = \frac{CL}{R_B} \cdot f_e \tag{3}$$

The CL_R in patients with moderate and severe CKD was compared with those in HV, and the RPs in each disease stage were obtained in the same manner as f_p and V_{ss}.

For alterations in CL_{intH}, as enough data of intravenous PK profiles in hepatically cleared drugs were not available, RPs were obtained from dose-normalized AUC after oral dosing in the 1st dataset. The theory underlying this calculation was derived from the well-stirred liver model and shown by the following equation:

$$\begin{aligned} AUC/Dose &= \frac{F_a \cdot F_g \cdot F_h}{CL} = \frac{F_a \cdot F_g \cdot (1-CL_H/Q_H)}{CL_H \cdot R_B/(1-f_e)} \\ &= \frac{F_a \cdot F_g \cdot (1-f_e)}{R_B} \cdot \frac{Q_H/(Q_H + CL_{intH})}{Q_H \cdot CL_{intH}/(Q_H + CL_{intH})} \\ &= \frac{F_a \cdot F_g \cdot (1-f_e)}{R_B \cdot CL_{intH}} \end{aligned} \tag{4}$$

$$\therefore CL_{intH} = \frac{F_a \cdot F_g \cdot (1-f_e)}{R_B \cdot AUC/Dose} \tag{5}$$

where Q_H is the hepatic blood flow, F_a is the fraction moving into enterocytes, F_g is the fraction escaping gut-wall elimination, and F_h is the fraction escaping hepatic elimination. Assuming that F_a, F_g, and R_B were not altered in the CKD condition, the RP of CL_{intH} was obtained as shown by the following equation:

$$\frac{CL_{intH,CKD}}{CL_{intH,HV}} = \frac{\dfrac{F_a \cdot F_g \cdot \left(1-f_{e,CKD}\right)}{R_B \cdot AUC_{CKD}/Dose}}{\dfrac{F_a \cdot F_g \cdot \left(1-f_{e,HV}\right)}{R_B \cdot AUC_{HV}/Dose}} = \frac{AUC_{HV}/Dose}{AUC_{CKD}/Dose} \cdot \frac{1-f_{e,CKD}}{1-f_{e,HV}} \tag{6}$$

Finally, RPs for CL_{UintH} were calculated using the corresponding mean RP for the f_p of acidic, basic, and neutral drugs under moderate and severe CKD conditions obtained in this study as shown in the following equation:

$$\frac{CL_{UintH,CKD}}{CL_{UintH,HV}} = \frac{CL_{intH,CKD}/f_{p,CKD}}{CL_{intH,HV}/f_{p,HV}} = \frac{CL_{intH,CKD}}{CL_{intH,HV}} \div \text{Mean RP for } f_p \tag{7}$$

The RPs in CL_R and CL_{UintH} were obtained from compounds with f_e values of >0.4 (mainly eliminated *via* the kidney) and <0.4 (mainly eliminated *via* the liver), respectively.

Prediction of CL in CKD Patients

The predictabilities for CLs in CKD condition were validated with the 2nd dataset. The SF for CL_R, f_p, and CL_{UintH} in patients with moderate and severe CKD, which represent the relative difference under the disease conditions compared to HV, was obtained as follows. The SF for CL_R was defined as the relative changes of GFR ranges under each disease condition. Although GFR is generally defined as a range of 15 to 30 mL/min/1.73 m^2 for severe CKD, the lower limit of 10 mL/min/1.73 m^2 was used for the calculation of SF, because patients with GFR below 15 mL/min/1.73 m^2 were often included in this survey. For HV, a GFR of 125 mL/min/1.73 m^2 was used for calculation (19). The SFs for f_p and CL_{UintH} were assumed to be equal to the interquartile ranges of the RP of each parameter in the disease states obtained in this study. The parameters under disease conditions ($CL_{R,CKD}$, $f_{p,CKD}$, and $CL_{UintH,CKD}$) were calculated by multiplying those under healthy conditions by the SFs.

To predict CL_H under CKD conditions ($CL_{H,CKD}$), the following simple well-stirred equation incorporating $f_{p,CKD}$ and $CL_{UintH,CKD}$ was used:

$$CL_{H,CKD} = \frac{Q_H \cdot \dfrac{f_{p,CKD}}{R_B} \cdot CL_{UintH,CKD}}{Q_H + \dfrac{f_{p,CKD}}{R_B} \cdot CL_{UintH,CKD}} \tag{8}$$

It was assumed that Q_H and R_B values are not altered under CKD conditions. By combining these $CL_{R,CKD}$ and $CL_{H,CKD}$, the total CL under the disease condition (CL_{CKD}) was predicted as expressed by the following equation:

$$CL_{CKD} = \left(CL_{R,CKD} + CL_{H,CKD}\right) \cdot R_B \tag{9}$$

Prediction of Plasma Concentrations in CKD Patients

Within the 2nd dataset, the compounds, for which plasma concentration-time profiles after intravenous dosing were available, were used for the validation of a PBPK model combined with the SFs in CKD patients. The structure of the PBPK model and physiological parameters used are shown in Supplementary Fig. S1 and Supplementary Table S3, respectively. The framework of the PBPK model had previously been reported (20), that is, the model is composed of 11 tissue compartments (lungs, adipose tissue, bones, brain, heart, muscles, kidneys, spleen, liver, skin, and small intestine), which are linked by venous and arterial blood pools. Perfusion rate-limited kinetics were assumed, and each tissue was represented by a single well-stirred compartment. The liver and kidney were considered as the elimination sites. The principles of mass balance equations for non-eliminating tissues, liver, and kidney are indicated by the following differential equations:

$$\frac{dC_T}{dt} \cdot V_T = Q_T \cdot \left(C_a - \frac{C_T}{K_{pT}/R_B}\right) \tag{10}$$

$$\frac{dC_H}{dt}\cdot V_H = Q_H\cdot C_a + Q_{SP}\cdot\frac{C_{SP}}{K_{pSP}/R_B} + Q_{SI}\cdot\frac{C_{SI}}{K_{pSI}/R_B} - (Q_H + Q_{SP} + Q_{SI})\cdot\frac{C_H}{K_{pH}/R_B} - \frac{f_p}{R_B}\cdot CL_{UintH}\cdot\frac{C_H}{K_{pH}/R_B} \quad (11)$$

$$\frac{dC_R}{dt}\cdot V_R = Q_R\cdot\left(C_a - \frac{C_R}{K_{pR}/R_B}\right) - CL_R\cdot C_a \quad (12)$$

where V is the volume, Q is the blood flow, C is the concentration, K_p is the tissue to plasma concentration ratio, and for subscripts, T is for tissue, a is for artery, H is for hepatic, SP is for spleen, SI is for small intestine, and R is for renal.

Firstly, the PBPK model was constructed using the observed f_p, CL_{UintH}, and CL_R to simulate the plasma concentration-time profiles after intravenous dosing in HV. The K_p values for HV in each tissue was calculated by the tissue composition-based equations proposed by Rodgers *et al.* (21,22), using clogP, pK_a, and f_p. A uniform factor obtained from the comparison of the predicted and observed V_{ss} was applied to the calculated K_p values for the adjustment of PK profiles in HV (20). The SFs for f_p, CL_{UintH}, and CL_R were then introduced to obtain the parameters under CKD conditions, and the plasma concentrations in patients were simulated. Note that the K_p values of CKD patients were recalculated by the same procedure using $f_{p,CKD}$.

The PK parameters (V_{ss}, CL, and $t_{1/2}$) were estimated by the non-compartmental analysis of simulated plasma concentrations in both HV and patients, and RP of these parameters in disease states were calculated. Model construction, simulation of plasma concentrations, and non-compartmental analysis were performed by Phoenix WinNonlin, version 6.3 (Pharsight, CA, USA).

RESULTS

Alterations of f_p and V_{ss} in CKD Patients

The RPs of f_p and V_{ss} in CKD patients compared with HV are shown in Fig. 1 and are summarized in Table I. For acidic and neutral compounds, the f_p increased in CKD patients with the median RP of 109 to 115% for moderate and 134 to 135% for severe CKD, indicating that the extent of change in the f_p depended on the progression of disease. On the contrary, the f_p for basic drugs showed no significant changes with the median RP of 99 to 104%. For the V_{ss}, no pronounced differences between the disease states or drug properties were observed with the median RP of 95 to 107%. The interquartile ranges of the RP for the obtained f_p in each class of drug presented in Table I were used as the SFs for the prediction of CL, CL_R, CL_H, and PK in CKD patients. Given that the alteration of V_{ss} was not found under any disease conditions and the V_{ss} was generally determined by the f_p and physicochemical properties in PBPK models, the SF of V_{ss} was not taken into consideration for PK prediction.

Alteration of CL_R in CKD Patients

The RPs of CL_R in CKD patients compared with HV are shown in Fig. 2 and Table II. The CL_R showed a disease state-dependent reduction with median RP of 31% for moderate

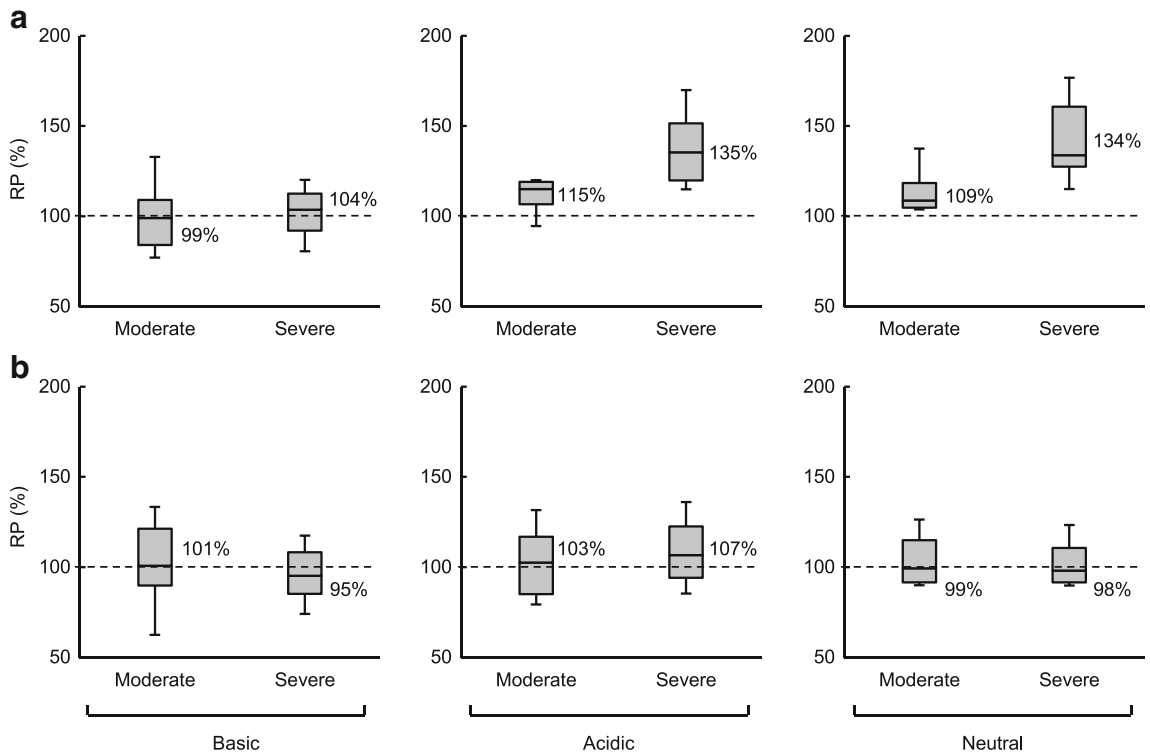

Fig. 1. RP of f_p (**a**) and V_{ss} (**b**) in moderate and severe CKD. In the boxes, the *middle lines* represent the median values, the *top* and *bottom margins* represent the 75th and 25th percentiles, and the *top* and *bottom whiskers* represent the 90th and 10th percentiles. The percentages on the *right* of the boxes represent median values

Table I. Alteration of f_p and V_{ss} in Moderate and Severe CKD

Parameter	CKD stage	Group	*n*	RP (%)			
				Median	(Interquartile range)	Mean	(SD)
f_p	Moderate	Basic	28	99	(84–109)	100	(23)
		Acidic	13	115	(107–119)	112	(12)
		Neutral	10	109	(105–118)	118	(25)
	Severe	Basic	26	104	(92–113)	103	(21)
		Acidic	16	135	(120–151)	139	(25)
		Neutral	10	134	(127–161)	147	(39)
V_{ss}	Moderate	Basic	13	101	(90–121)	103	(32)
		Acidic	17	103	(85–117)	104	(23)
		Neutral	10	99	(92–115)	109	(26)
	Severe	Basic	17	95	(85–108)	99	(28)
		Acidic	19	107	(94–123)	110	(27)
		Neutral	12	98	(92–111)	107	(28)

CKD chronic kidney disease, *RP* relative percentage, f_p unbound fraction in plasma, V_{ss} volume of distribution at a steady state

and 12% for severe CKD. The alterations in CL_R were within the range of change for GFR (24 to 47% for moderate and 8 to 23% for severe CKD). Compounds with lower and higher unbound CL_R (CL_R/f_B) than GFR, which can be considered to be predominantly eliminated by glomerular filtration and tubular secretion, respectively, showed similar changes in the CL_R, as determined by the median RP of 35 *versus* 31% for moderate and 13 *versus* 11% for severe CKD. This finding indicated that the alterations in CL_R can be predicted based on the GFR regardless of the elimination mechanism. Therefore, instead of the interquartile ranges of the RP of CL_R, the ranges of GFR to be defined in moderate and severe CKD were applied as the SF for the prediction of CL_R and PK in CKD patients.

Alteration of CL_{UintH} in CKD Patients

The RPs for CL_{UintH} in CKD patients compared with HV were obtained from the 1st dataset and are shown in Fig. 3 and Table II. In both disease stages, a similar extent of decrease in CL_{UintH} was noted for CYP and UDP-glucuronosyltransferase (UGT) substrates and drugs eliminated *via* other mechanisms, with the median RP of 67 to 68% in moderate and 59 to 65% in severe CKD conditions. The change in CL_{UintH} was unlikely dependent both on the disease stage of CKD and the elimination mechanism in the liver. Consequently, the median RP of CL_{UintH} for all examined drugs was calculated as 68% (interquartile range, 55 to 82%) in moderate and 62% (interquartile range 48 to 80%) in severe CKD, and these interquartile ranges were used as the SFs for the following predictions of CL_H and PK in CKD patients.

Prediction of CLs in CKD Patients

The present study demonstrated that there were relatively large variations in the alterations of CL_R and CL_H between the examined compounds, and therefore, CLs in the 2nd dataset were predicted using SFs based on the interquartile ranges analyzed for the CL_{UintH} and f_p. The SFs for CL_R, CL_{UintH}, and f_p used in the present study are summarized in Table III. The predicted and observed mean RP of CL_R, CL_H, and CL in CKD patients compared with HV and the success rates of the prediction are shown in Table IV. The predicted mean RPs were in good agreement with the observed values for CL_R (36 *vs* 43% in moderate and 16 *vs* 21% in severe CKD), CL_H (75 *vs* 73% in moderate and 79 *vs* 69% in severe CKD) and CL (54 *vs* 52% in moderate and 45

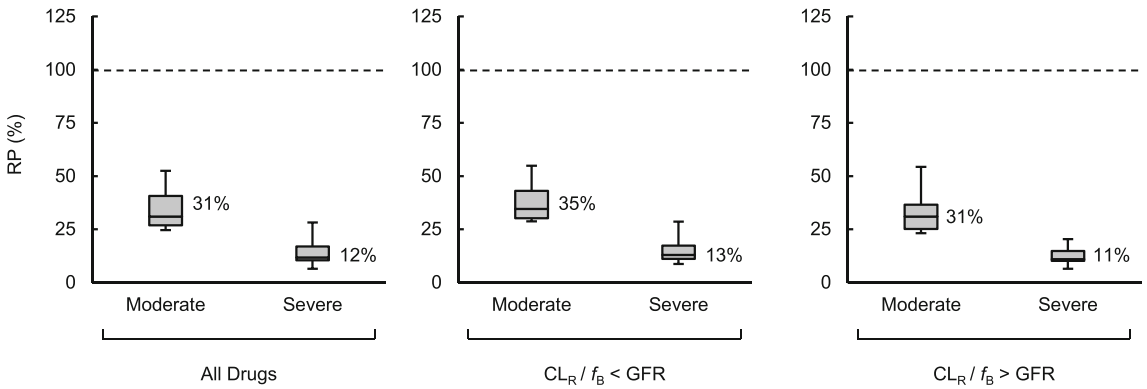

Fig. 2. RP of CL_R in moderate and severe CKD. In the boxes, the *middle lines* represent the median values, the *top* and *bottom margins* represent the 75th and 25th percentiles, and the *top* and *bottom whiskers* represent the 90th and 10th percentiles. The percentages on the *right* of the boxes represent median values

Table II. Alteration of CL_R and CL_{UintH} in Moderate and Severe CKD

Parameter	CKD stage	Group	*n*	RP (%) Median	(Interquartile range)	Mean	(SD)
CL_R	Moderate	All drugs	25	31	(27–41)	36	(14)
		CL_R/f_B<GFR	10	35	(30–43)	39	(12)
		CL_R/f_B>GFR	15	31	(25–37)	34	(15)
	Severe	All drugs	25	12	(10–17)	14	(8)
		CL_R/f_B<GFR	11	13	(11–17)	16	(9)
		CL_R/f_B>GFR	14	11	(10–15)	13	(6)
CL_{UintH}[a]	Moderate	All drugs	64	68	(55–82)	69	(20)
		CYP substrates	36	68	(56–89)	72	(22)
		UGT substrates	11	67	(61–86)	69	(16)
		Others	17	68	(53–76)	63	(16)
	Severe	All drugs	68	62	(48–80)	64	(21)
		CYP substrates	42	65	(48–80)	66	(23)
		UGT substrates	10	59	(47–68)	59	(16)
		Others	16	60	(51–72)	63	(19)

CKD chronic kidney disease, *RP* relative percentage, CL_R renal blood clearance, CL_{UintH} unbound intrinsic clearance, f_B unbound fraction in blood, *GFR* glomerular filtration rate, *UGT* UDP-glucuronosyltransferase, *CYP* cytochrome P450
[a] RPs of CL_{UintH} were obtained from the 1st dataset

vs 43% in severe CKD). When the range of the predicted CLs included the observed data, the prediction was defined to be successful. The percentages of compounds that were successfully predicted were 66 to 70% for CL_R, 47 to 48% for CL_H, and 67 to 68% for CL.

Prediction of Plasma Concentrations in CKD Patients

The plasma concentration-time profiles after intravenous dosing of 12 model compounds in HV, moderate, and severe CKD were simulated by the PBPK model incorporating the

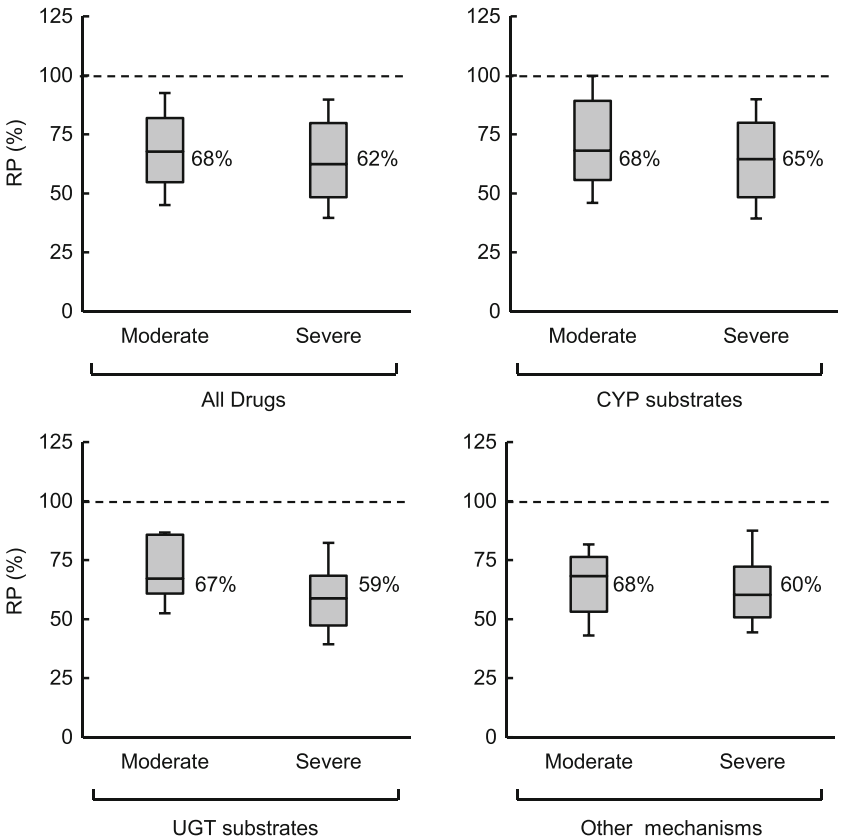

Fig. 3. RP of CL_{UintH} in moderate and severe CKD obtained from the 1st dataset. In the boxes, the *middle lines* represent the median values, the *top and bottom margins* represent the 75th and 25th percentiles, and the *top and bottom whiskers* represent the 90th and 10th percentiles. The percentages on the *right* of the boxes represent median values

Table III. SFs for CL_R, CL_{UintH}, and f_p for the Prediction of CL and PK in CKD

Parameter	Group	Moderate CKD (%)	Severe CKD (%)
CL_R	All drugs	24–47	8–23
CL_{UintH}	All drugs	55–82	48–80
f_p	Basic	84–109	92–113
	Acidic	107–119	120–151
	Neutral	105–118	127–161

CKD chronic kidney disease, CL_R renal blood clearance, CL_{UintH} unbound intrinsic clearance, f_p unbound fraction in plasma

SFs under the disease conditions. The predicted range and mean observed RP for CL, V_{ss}, and $t_{1/2}$ in CKD patients are summarized in Table V. The simulated plasma concentration-time curves of six drugs (the best and worst predicted compounds in each group; mainly eliminated *via* the renal, non-renal, and mixed routes) are also described in Fig. 4. In case the range of the predicted parameters included the observed values, the compounds were classified as showing successful prediction. For the CL prediction in CKD patients, 10 (83%) and 7 (58%) of 12 compounds were regarded to show successful prediction in moderate and severe CKD, respectively. The alterations of $t_{1/2}$ in CKD patients were also well-predicted by the PBPK model, accompanied with successful predictions in 9 (75%) and 8 (67%) of 12 compounds under moderate and severe CKD conditions, respectively.

DISCUSSION

In the present study, we extensively collected clinical data of 151 compounds with various pharmacokinetic properties and analyzed the impact of CKD on different PK parameters. Notably, for altered hepatic elimination, clinical data of over 70 compounds were comprehensively analyzed. The CL_{UintH} of compounds that are eliminated *via* hepatic metabolism by CYP, UGT, or other mechanisms decreased to a similar extent in CKD patients as to HV. CL_R showed a similar decrease to GFR irrespective of the involvement of tubular secretion. The RP in each parameter under different disease conditions showed large variations, which might involve a variety of mechanisms. Therefore, SFs based on the interquartile range estimated by a statistical analysis of the RP were applied to the well-stirred model to predict the CLs in CKD patients. CL_H and CL_R were successfully predicted for approximately half and two-thirds of the compounds, respectively. Importantly, the SFs for CL_{UintH} obtained from the 1st dataset were validated using the different datasets (the 2nd dataset) in the prediction of CLs. The plasma concentration-time curves of 12 model compounds in CKD patients were also well-predicted by the application of the SFs into the PBPK model, as demonstrated by the relatively high success rates for CL and $t_{1/2}$.

During the drug development stage, a perspective evaluation for the influence of CKD on the PK of new molecular entities has become a critical issue for the pharmaceutical industries. Since multiple factors are complexly intertwined in the alteration of the PK under CKD conditions, we employed the top-down approach rather than the bottom-up approach based on *in vitro* and *in silico* data. Some authors have proposed PBPK models incorporating the CL_{UintH} reduction in CKD patients based on the top-down approach; however, these models were derived from a limited number of clinical data (13–15). On the other hand, one advantage of this study is that SFs based on an interquartile range derived from a relatively large number of clinical data are employed and would have a possibility for encompassing widely ranging PK alterations by various mechanisms in CKD.

Plasma protein binding is a governed factor to PK behavior and is known to vary depending on the plasma concentrations of the binding proteins as well as several other factors in CKD patients such as the competition of the binding sites by metabolites that have accumulated as a result of reduced renal function or the denaturation of albumin itself due to uremic toxins (23). Strougo *et al.* demonstrated that the albumin plasma concentration tended to decrease, but the median α_1-acid glycoprotein level in the plasma was 1.4 times higher in patients with moderate to severe CKD compared to the control group (15). In this study, acidic and neutral compounds clearly exhibited an increase in f_p in patients with severe CKD probably due to a decrease in the plasma concentration of albumin to which these classes of compounds mainly bind (24). Regarding basic compounds, it

Table IV. Predicted and Observed RP of CLs in CKD Patients and Success Rates of the Prediction

			Mean RP (%)		Success rate (%)		
CKD stage	Parameter	*n*	Observed	Predicted	Successfully predicted[a]	Over-predicted[b]	Under-predicted[c]
Moderate	CL	34	52	54	68	12	21
	CL_R	32	43	36	66	22	13
	CL_H	33	73	75	48	18	33
Severe	CL	36	43	45	67	8	25
	CL_R	33	21	16	70	21	9
	CL_H	34	69	79	47	15	38

The predictabilities for CLs were evaluated using the 2nd dataset
CKD chronic kidney disease, *RP* relative percentage, *CL* clearance, CL_R renal blood clearance, CL_H hepatic clearance
[a] The predicted range included the observed change
[b] The predicted range was greater than the observed change
[c] The predicted range was smaller than the observed change

Table V. Predicted and Observed RP of CL, V_{ss}, and $t_{1/2}$ in 12 Model Compounds in CKD by the PBPK Model

			CL		V_{ss}		$t_{1/2}$	
Disease stage	Compound	f_e	Observed	Predicted	Observed	Predicted	Observed	Predicted
Moderate CKD	Isepamicin	1	*40*	24–47	171	98–105	*387*	208–438
	Zanamivir	0.90	*38*	28–52	*101*	101–105	*234*	199–363
	Cefepime	0.88	*37*	28–53	129	99–103	*307*	193–350
	Cidofovir	0.86	26	29–54	115	101–102	468	182–330
	Enprofylline	0.82	*32*	31–56	74	105–113	*226*	185–298
	Carumonam	0.78	*41*	32–58	117	104–110	*220*	185–315
	Meropenem	0.77	*39*	32–56	111	101–102	*251*	175–301
	Tomopenem	0.57	*34*	34–65	*105*	89–120	365	135–344
	Cefotetan	0.49	*46*	43–73	99	101–103	*193*	141–236
	Batanopride	0.20	94	52–84	121	96–110	*121*	109–179
	Cyclophosphamide	0.19	*71*	54–87	121	104–113	*188*	130–191
	Lidocaine	0	*77*	67–95	101	97–99	135	101–134
Severe CKD	Isepamicin	1	*20*	8–23	184	98–103	*944*	424–1,252
	Zanamivir	0.90	*23*	13–34	*108*	107–115	*425*	336–784
	Cefepime	0.88	*22*	14–35	139	102–110	*574*	313–722
	Cidofovir	0.86	11	15–37	93	103–105	842	274–641
	Enprofylline	0.82	8	17–40	71	114–135	797	298–564
	Carumonam	0.78	*21*	19–39	102	111–112	*416*	275–562
	Meropenem	0.77	*23*	18–37	117	102–102	*463*	261–535
	Tomopenem	0.57	17	24–51	78	88–110	*366*	170–452
	Cefotetan	0.49	*33*	33–72	87	104–109	*209*	150–307
	Batanopride	0.20	*63*	47–80	*98*	95–106	*177*	111–190
	Cyclophosphamide	0.19	44	49–81	92	113–114	241	139–229
	Lidocaine	0	45	65–96	88	96–97	192	99–136

Values in italic form represent successfully predicted cases
CKD chronic kidney disease, *RP* relative percentage, f_e fraction excreted unchanged in urine, *CL* clearance, V_{ss} volume of distribution at a steady state, $t_{1/2}$ elimination half-life

was assumed that f_p would decrease if the α_1-acid glycoprotein plasma level increases in severe CKD in theory; but in practice, the f_p of some compounds almost remained constant or increased in moderate and severe CKD, which is probably due to multiple mechanisms. Importantly, V_{ss} was almost consistent for all of the examined compounds regardless of the increase of f_p in acidic and neutral drugs possibly because these classes of compounds have relatively small distribution volume which is not sensitive to the alteration of plasma protein binding.

In general, the renal tubular secretion is reportedly known to involve various transporters including organic anion transporters 1 (OAT1) and 3 (OAT3), organic cation transporter 2 (OCT2), and multidrug resistance protein 2 (MRP2) (25). An animal study using CRF rats demonstrated the alteration of hepatic and intestinal protein expression levels of multidrug resistance 1 (MDR1) and MRP2 (4). However, there is no literature on the up- or down-regulation of proteins or mRNA expression levels of those transporters in the kidneys of CKD patients. Interestingly, the impact of CKD on glomerular filtration and on renal tubular secretion was not different, and the RP of CL_R for compounds that undergo tubular secretion was proportional to GFR. This finding provides insight into CL_R prediction, namely that GFR is still a dominant factor to predict CL_R regarding renal tubular secretion in addition to glomerular filtration.

Unexpectedly, the percentage reduction of CL_{UintH} in CKD patients relative to that in HV was not affected by the disease progress and was within a similar range for CYP and UGT substrates. The result was in agreement with the findings reported by Zhang *et al.*, who showed that there were no significant differences in the AUC changes between CYP and non-CYP substrates in CKD patients (6). In addition, the RPs of CL_{UintH} for typical substrates of CYP1A2, CYP2C9, and CYP3A did not differ in CKD patients except for CYP2D6 that slightly showed the lower RP (data not shown). Rowland *et al.* also evaluated the RPs for CYP1A, CYP2C9, CYP2D6, and CYP3A4 (13). The estimated RPs were decreased by the progression of the disease and appeared to be slightly lower than the corresponding median data in our study. In hepatocytes prepared from rats with CRF, down-regulation was found for CYP2C11 and CYP3A1/2, but not for CYP1A2 and CYP2D proteins (26). There may be species differences in the down-regulation of CYP enzymes between humans and rats. It has not yet been attempted to investigate a change in UGT expression level by the CRF condition in preclinical studies.

One of our objectives of this study was to acquire SFs based on a relatively large amount of clinical data to develop a universal prediction model by the top-down approach. To increase the number of compounds, the RP for the reduction of hepatic elimination was estimated from the oral AUC, which was in contrast to Rowland's method using a small number of intravenous PK data (13). The alterations of CL_{UintH} under CKD conditions were evaluated assuming that the F_a and F_g are not affected by CKD. The F_a and F_g are controlled by passive absorption, transporter-mediated influx and efflux, and metabolism mainly by CYP3A in humans. It

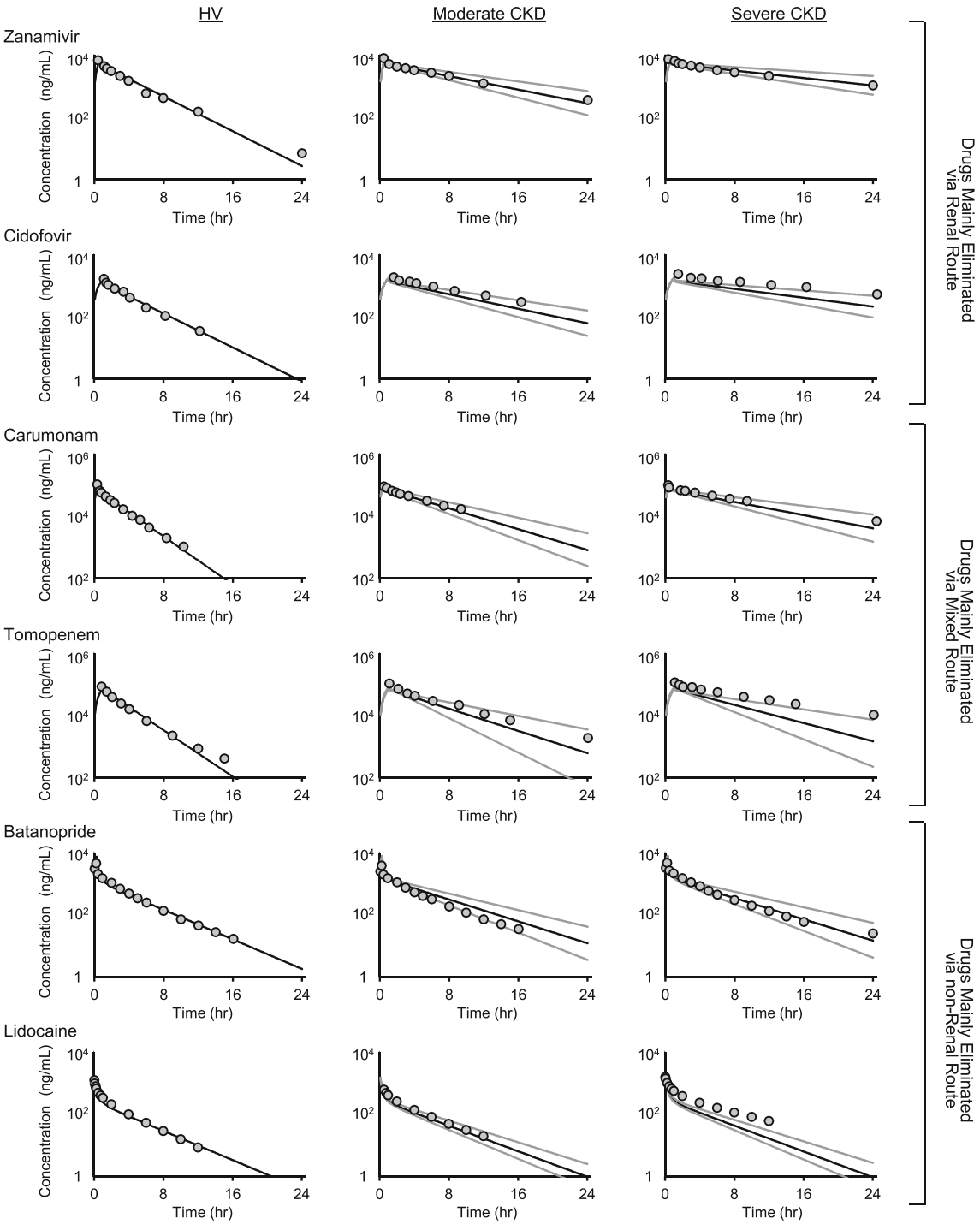

Fig. 4. Examples of plasma concentration-time simulations after intravenous dosing in HV and CKD conditions by the PBPK model combined with SFs. The *black lines* represent averaged predicted curves. The *gray lines* represent the predicted ranges of plasma concentrations. The *gray circles* are observed concentrations of each model compound. Best (zanamivir, carumonam, batanopride) and worst (cidofovir, tomopenem, lidocaine) cases of prediction in each group of drugs mainly eliminated *via* renal route, mixed route and non-renal route are presented

has been reported that P-glycoprotein and some CYP enzymes including CYP3A are down-regulated in the small intestine of animal models of CRF (27,28), which leads to the increase of F_a and F_g in the disease condition. CYP3A substrates among our dataset were regarded as relatively high F_h compounds, and this implied that F_g of these compounds were also high and that the effect of the alternation of F_g on the estimation of SF was limited. It is important to note that the applicability of SFs derived from the oral AUC was proven by a relatively high success rate for CL in different datasets after intravenous dosing, which shows a minor effect of the alterations of F_a and/or F_g on RPs' estimation. In this

study, however, as PK alterations of midazolam, which is known as the typical substrate of CYP3A with a significant intestinal first-pass metabolism (29), could not be evaluated because both moderate and severe CKD data were not separately available, further discussion would be needed for the effect of the alteration of F_g in the disease conditions.

Another assumption in obtaining the SF for CL_{UintH} is that R_B value does not change in the disease condition. Since R_B is a function of f_p which increased by up to approximately 50% in neutral drugs in the disease condition, the alteration of R_B could have an impact on the determination of SF for CL_{UintH}. However, relatively high plasma protein binding of drugs in the 1st dataset (averaged value of known f_p, 0.11) indicated low distribution to blood cell, and the impact of the change of R_B on SF seems to be minor. In addition, regarding compounds that strongly bind to α_1-acid glycoprotein, the change of f_p due to increased plasma binding protein level in the disease condition would give an impact to SF for CL_{UintH}. Further analysis on the alteration of f_p in patients would be required for such compounds.

Some drugs are known to be mainly eliminated *via* hepatic transporters such as organic anion transporting polypeptides (OATPs) (30), but the number of such compounds included in the current dataset was so limited. Consequently, the estimated SF is unlikely to reflect a change in the hepatic uptake activity; hence, the insufficient dataset for the liver uptake *via* transporters could be one of the reasons for the over-prediction of CL.

The PBPK model with SFs based on an interquartile range estimated in the present study was used for the simulation of the plasma concentration profiles of 12 model compounds with widely ranging f_e values. Consequently, the plasma concentrations of the 12 model drugs seemed to coincide with the observed data, and this was supported by a relatively high accuracy of CL and $t_{1/2}$, which were successfully predicted for 58 to 83% and 67 to 75% compounds, respectively, in CKD patients. These data suggest the utility of SFs with an interquartile range on PK prediction in CKD patients of drugs eliminated by different pathways. For the prediction of V_{ss}, only two compounds in each moderate and severe CKD condition were successfully predicted. Since the prediction of V_{ss} is based on the alteration of f_p in the PBPK model, an improved prediction method of f_p in disease condition would lead to a better predictability of V_{ss}.

More recently, translational research, which involves the translation of efficacy and PK data from preclinical to clinical studies *via* modeling and simulation cycles, occupies an important position in drug development (31,32). We have proposed the tiered approach, which consists of four steps based on modeling and simulation of PBPK models to predict human PK from drug discovery to first-in-human studies (20). In the last step, the measured plasma concentration profile in HV allows us to optimize the PBPK model by the integration of comprehensive *in vitro* and *in vivo* information. Such a PBPK model developed through modeling and simulation would become a key tool to evaluate intrinsic factors (age, gender, race, disease, and genetic polymorphism) on human PK in clinical studies. In the draft guidance, FDA recommends that pharmaceutical companies conduct either "the reduced PK study" in end-stage renal disease patients or "the full PK study" for more detailed evaluation in mild, moderate, and severe CKD patients to assess the possible impact of CKD on drug disposition under development (7). The new method with SFs derived by the top-down approach would provide a rationale for the selection of the appropriate study as well as dose adjustment through predicting the PK profile in patients from that in HV and also accelerates the implementation of model-based drug development that is deeply associated with decision-making based on PK profile prediction and risk assessment of toxicity.

CONCLUSION

We collected the large dataset regarding PK parameters in CKD patients and comprehensively described large variations in the alterations in PK parameters. Consequently, the SFs with an interquartile range were successfully derived from PK parameters in the disease conditions by the top-down approach. The predictability of the PBPK model combined with the SFs was validated using 12 model compounds with various PK profiles. The developed PBPK model with information on SFs would play an important role in the translational research in drug development.

REFERENCES

1. Coresh J, Selvin E, Stevens LA, Manzi J, Kusek JW, Eggers P, *et al.* Prevalence of chronic kidney disease in the United States. JAMA. 2007;298:2038–47.
2. 2013 USRDS annual data report. Available from: www.usrds.org/adr.aspx.
3. Dreisbach AW. The influence of chronic renal failure on drug metabolism and transport. Clin Pharmacol Ther. 2009;86:553–6.
4. Nolin TD, Naud J, Leblond FA, Pichette V. Emerging evidence of the impact of kidney disease on drug metabolism and transport. Clin Pharmacol Ther. 2008;83:898–903.
5. Sun H, Frassetto L, Benet LZ. Effects of renal failure on drug transport and metabolism. Pharmacol Ther. 2006;109:1–11.
6. Zhang Y, Zhang L, Abraham S, Apparaju S, Wu TC, Strong JM, *et al.* Assessment of the impact of renal impairment on systemic exposure of new molecular entities: evaluation of recent new drug applications. Clin Pharmacol Ther. 2009;85:305–11.
7. Draft guidance for industry: pharmacokinetics in patients with impaired renal function—study design, data analysis, and impact on dosing and labeling (2010). Available from: www.fda.gov/downloads/Drugs/GuidanceComplianceRegulatoryInformation/Guidances/ucm204959.pdf.
8. Zhao P, Zhang L, Grillo JA, Liu Q, Bullock JM, Moon YJ, *et al.* Applications of physiologically based pharmacokinetic (PBPK) modeling and simulation during regulatory review. Clin Pharmacol Ther. 2011;89:259–67.
9. Edginton AN, Willmann S. Physiology-based simulations of a pathological condition: prediction of pharmacokinetics in patients with liver cirrhosis. Clin Pharmacokinet. 2008;47:743–52.
10. Johnson TN, Boussery K, Rowland-Yeo K, Tucker GT, Rostami-Hodjegan A. A semi-mechanistic model to predict the effects of liver cirrhosis on drug clearance. Clin Pharmacokinet. 2010;49:189–206.
11. Belpaire FM, Rosseel MT, Vermeulen AM, De Smet F, Bogaert MG. Stereoselective pharmacokinetics of atenolol in the rat: influence of aging and of renal failure. Mech Ageing Dev. 1993;67:201–10.
12. Mukai H, Morino A. Effects of renal insufficiency and aging on the pharmacokinetics of a phenethylamine class alpha(1A)-adrenoceptor agonist NS-49. Int J Pharm. 1999;185:37–43.

13. Rowland Yeo K, Aarabi M, Jamei M, Rostami-Hodjegan A. Modeling and predicting drug pharmacokinetics in patients with renal impairment. Expert Rev Clin Pharmacol. 2011;4:261–74.
14. Zhao P, Vieira Mde L, Grillo JA, Song P, Wu TC, Zheng JH, *et al*. Evaluation of exposure change of nonrenally eliminated drugs in patients with chronic kidney disease using physiologically based pharmacokinetic modeling and simulation. J Clin Pharmacol. 2012;52(1 Suppl):91S–108.
15. Strougo A, Yassen A, Krauwinkel W, Danhof M, Freijer J. A semiphysiological population model for prediction of the pharmacokinetics of drugs under liver and renal disease conditions. Drug Metab Dispos. 2011;39:1278–87.
16. Akabane T, Tabata K, Kadono K, Sakuda S, Terashita S, Teramura T. A comparison of pharmacokinetics between humans and monkeys. Drug Metab Dispos. 2010;38:308–16.
17. Nakamori F, Naritomi Y, Hosoya K, Moriguchi H, Tetsuka K, Furukawa T, *et al*. Quantitative prediction of human intestinal glucuronidation effects on intestinal availability of UDP-glucuronosyltransferase substrates using in vitro data. Drug Metab Dispos. 2012;40:1771–7.
18. Poulin P, Theil FP. Prediction of pharmacokinetics prior to in vivo studies. 1. Mechanism-based prediction of volume of distribution. J Pharm Sci. 2002;91:129–56.
19. Davies B, Morris T. Physiological parameters in laboratory animals and humans. Pharm Res. 1993;10:1093–5.
20. Sayama H, Komura H, Kogayu M, Iwaki M. Development of a hybrid physiologically based pharmacokinetic model with drug-specific scaling factors in rat to improve prediction of human pharmacokinetics. J Pharm Sci. 2013;102:4193–204.
21. Rodgers T, Leahy D, Rowland M. Physiologically based pharmacokinetic modeling 1: predicting the tissue distribution of moderate-to-strong bases. J Pharm Sci. 2005;94:1259–76.
22. Rodgers T, Rowland M. Physiologically based pharmacokinetic modelling 2: predicting the tissue distribution of acids, very weak bases, neutrals and zwitterions. J Pharm Sci. 2006;95:1238–57.
23. Dreisbach AW, Lertora JJ. The effect of chronic renal failure on drug metabolism and transport. Expert Opin Drug Metab Toxicol. 2008;4:1065–74.
24. Kwong TC. Free drug measurements: methodology and clinical significance. Clin Chim Acta. 1985;151:193–216.
25. Inui KI, Masuda S, Saito H. Cellular and molecular aspects of drug transport in the kidney. Kidney Int. 2000;58:944–58.
26. Leblond F, Guévin C, Demers C, Pellerin I, Gascon-Barré M, Pichette V. Downregulation of hepatic cytochrome P450 in chronic renal failure. J Am Soc Nephrol. 2001;12:326–32.
27. Leblond FA, Petrucci M, Dubé P, Bernier G, Bonnardeaux A, Pichette V. Downregulation of intestinal cytochrome p450 in chronic renal failure. J Am Soc Nephrol. 2002;13:1579–85.
28. Naud J, Michaud J, Boisvert C, Desbiens K, Leblond FA, Mitchell A, *et al*. Down-regulation of intestinal drug transporters in chronic renal failure in rats. J Pharmacol Exp Ther. 2007;320:978–85.
29. Komura H, Iwaki M. In vitro and in vivo small intestinal metabolism of CYP3A and UGT substrates in preclinical animals species and humans: species differences. Drug Metab Rev. 2011;43:476–98.
30. Shitara Y, Maeda K, Ikejiri K, Yoshida K, Horie T, Sugiyama Y. Clinical significance of organic anion transporting polypeptides (OATPs) in drug disposition: their roles in hepatic clearance and intestinal absorption. Biopharm Drug Dispos. 2013;34:45–78.
31. Huang SM, Abernethy DR, Wang Y, Zhao P, Zineh I. The utility of modeling and simulation in drug development and regulatory review. J Pharm Sci. 2013;102:2912–23.
32. Zhang L, Pfister M, Meibohm B. Concepts and challenges in quantitative pharmacology and model-based drug development. AAPS J. 2008;10:552–9.